Journal of ELECTRONIC MATERIALS, Vol. 44, No. 11, 2015
DOI: 10.1007/s11664-015-3930-2
© 2015 The Minerals, Metals & Materials Society

CrossMark

Electroless Silver Coating on Copper Microcones for Low-Temperature Solid-State Bonding

FENGTIAN HU,[1,2] SHAN YANG,[1] HAOZHE WANG,[1] ANMIN HU,[1,3] and MING LI[1,4]

1.—State Key Laboratory of Metal Matrix Composites, Key Laboratory for Thin Film and Microfabrication Technology of the Ministry of Education, School of Materials Science and Engineering, Shanghai Jiao Tong University, Shanghai 200240, People's Republic of China. 2.—e-mail: toyota211@sjtu.edu.cn. 3.—e-mail: huanmin@sjtu.edu.cn. 4.—e-mail: mingli90@sjtu.edu.cn

A low-temperature solid-state bonding technology using silver-coated Cu microcones and Sn-3.0Ag-0.5Cu (wt.%) solder for three-dimensional (3D) packaging is presented. Electroless silver coating on the surfaces of copper microcones effectively reduces oxide layer growth and significantly enhances the solder joint shear strength from an average of 33.5 MPa to 43.4 MPa. Low-temperature thermocompression bonding at 463 K in ambient air was achieved using silver-coated Cu microcones, with no voids found along the bonded interface. Microscopic observation revealed that the microcones were completely inserted into the soft solder. Probable mechanisms for this bonding process are proposed and discussed.

Key words: 3D integration, Cu microcones, silver coating, oxidation resistance, low-temperature bonding

INTRODUCTION

The high requirement for electronic products is driving the demand for high-density interconnection. Three-dimensional integrated circuits (3D ICs) have become the leading approach to obtain high package density, because they have tremendous potential to reduce global interconnect latency and power dissipation, since the solder bumps are smaller and the pitch finer. In particular, for high interconnection density, stacked bonding is gaining in popularity. Considered as one of the most important technical trends, stacked bonding is being widely developed to achieve the goal of 3D ICs,[1–3] due to its many advantages such as excellent electrical properties, intrinsic interconnect and high mechanical reliability, etc. Generally, direct Cu–Cu thermocompression bonding requires high-energy irradiation and extra surface-finishing processes such as polishing. However, high bonding pressure, a clean surface, and temperature up to 350°C to 400°C are always required to ensure the integrity of such bonding, thus limiting further applications of this technology.[4–7] It has been verified that such high temperature and pressure may also degrade device performance. Consequently, investigating low-temperature bonding technology is essential to reduce cost and process complexity.

Several researchers have carried out studies in this field. Zhang et al.[8] used Cu cones to enhance the interfacial adhesion between a Cu-based substrate and epoxy molding compound (EMC). Chen et al.[9,10] reported on low-temperature solid-state bonding using Ni microcones. Wang et al.[11] developed a room-temperature ultrasonic bonding process using Ni microcones. Moreover, a fluxless low-temperature insertion bonding method using Cu-based microcones as substrate was studied by Lu et al.[11] However, none of the systems investigated in these studies are ideal for actual application.

As is well known, the surface of copper is susceptible to oxidization during the packaging process due to its high affinity for oxygen.[12–14] In this research, we focus on the influences of different silver layer thicknesses on the oxidation behavior of Cu microcones. The shape of the Cu microcones remained unchanged after being coated with the

(Received April 21, 2015; accepted July 6, 2015; published online July 21, 2015)

silver layer for antioxidation. Insertion bonding technology between Cu microcones and solder at 463 K in ambient air is also explored. Comparing with other solid-state bonding methods, the shear strength and enhanced oxidation resistance of the presented method are discussed and elucidated. In addition, a probable mechanism is provided to understand this bonding process.

EXPERIMENTAL PROCEDURES

Synthesis of Copper Microcones and Ag Coating Layer

In this work, copper microcones were electroless plated onto 7 cm × 5 cm × 0.15 mm C194 copper sheets (Cu-2.35%Fe-0.03%P-0.1%Zn; Kobelco, Yamaguchi, Japan). First, Cu plates were degreased for 1 min electrochemically, acid-cleaned with 20% HCl for 20 s, and subjected to $PdCl_2$ activation for 60 s. After pretreatment, copper microcone arrays were electroless plated on the substrate in an electrobath. The electrolyte was composed of analytical pure $CuSO_4 \cdot 5H_2O$ (0.03 mol/L), $NiSO_4 \cdot 6H_2O$ (0.0024 mol/L), $NaH_2PO_2 \cdot H_2O$ (0.24 mol/L), $Na_3C_6H_5O_7 \cdot 2H_2O$ (0.05 mol/L), and H_3BO_3 (0.50 mol/L) as well as polyethylene glycol (5 ppm) as a crystallization modifier. The temperature was kept at 333 K, and the pH value was 8.5 to 9.0 (adjusted using 20% NaOH solution), as reported by Zhang et al.[15]

To prevent the copper microcone surface from being oxidized under the heating condition in the bonding process, we planned to electroless deposit a silver layer on its surface. Ag coating was electroless deposited on the surface of the as-prepared Cu microcones at 298 K, as reported by Zhao et al.[16] The electrolyte was composed of 40 g/L $AgNO_3$, 225 g/L $Na_2S_2O_3$, 40 g/L $K_2S_2O_5$, and crystal modifier. The current density was 0.2 A/dm^2, and the deposition time was varied from 0 min to 24 min.

Bonding Test and Shear Test

Sn-3.0Ag-0.5Cu (wt.%) solder ball (760 μm) was bonded to Cu microcones using a modified Rhesca PTR-1101 bonding tester. Figure 1 shows the bonding process schematically. Solder ball was put on the substrate with the Cu microcone layer. The loader started to exert vertical pressure. The ponding process lasted 3 min at temperature of 463 K with pressure of 1000 g on each ball. The whole bonding process was carried out below the melting point of Sn-3.0Ag-0.5Cu (wt.%) solder (491 K) to ensure that the whole welding process was carried out in the solid condition. Ball shear testing was performed using the same modified Rhesca PTR-1101 bonding tester after the complete bonding process, as reported previously.[9]

The surface morphologies of Cu microcones were observed by field-emission scanning electron microscopy (FE-SEM, FEI-Sirion 200). The compositions of the fracture and interface were measured using an Oxford Inca X-Act energy-dispersive spectrometer (EDS) incorporated into the FE-SEM. X-ray diffraction (XRD; Rigaku D/MAX-IIIA) analysis was used to identify the phases.

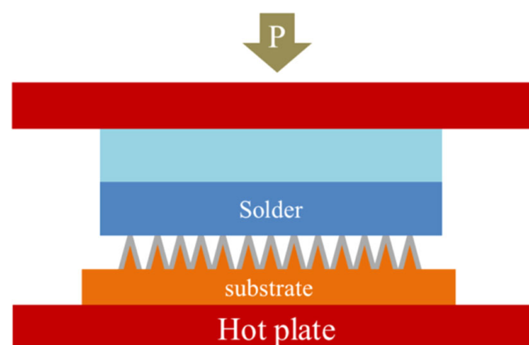

Fig. 1. Schematic diagram of bonding process.

X-ray fluorescence spectroscopy (XFS; Fischerscope X-ray XUL-XYm) measurements were carried out to measure the Ag layer thickness. Each result in this study is an average of three measurements of different regions to achieve more precise data.

The thickness of the oxide layer was measured using the cathodic reduction method. Heated samples were reduced at constant current density of 0.5 mA/cm^2 in 0.1 mol/L NaOH solution, and the oxide film thickness was calculated from the quantity of electricity needed to complete the whole reduction reaction.

RESULTS AND DISCUSSION

Morphological Observation

Figure 2 shows SEM images of the Ag layer on top of Cu microcones for different deposition times of electroless silver of 0 min, 6 min, 12 min, 18 min, and 24 min. As shown in Fig. 2a, the copper deposits were fine, dense, and uniform with typical cone shape. Figure 2b–e exhibits the morphological change of the Cu microcones coated with Ag as the deposition time was extended from 6 min to 24 min. The shape of the microcones remained basically unchanged. However, as the electroless plating time was increased, some microcones became round.

The relationship between the Ag layer thickness and the electroless deposition time is illustrated in Fig. 3. Under each condition, four specimens were tested for statistical accuracy. For specimens plated for 6 min, 12 min, 18 min, and 24 min, the average thickness for the four conditions was measured to be 0.15 μm, 0.35 μm, 0.43 μm, and 0.44 μm, respectively. It reached a maximum value of 0.44 μm when the deposition time was 24 min. With increasing deposition time, the thickness of the silver coating increased but the growth rate decreased. However, after 20 min, the thickness for longer time did not change significantly, eventually remaining at about 0.43 μm. This result indicates that the dissolution of the metal matrix occurred on the

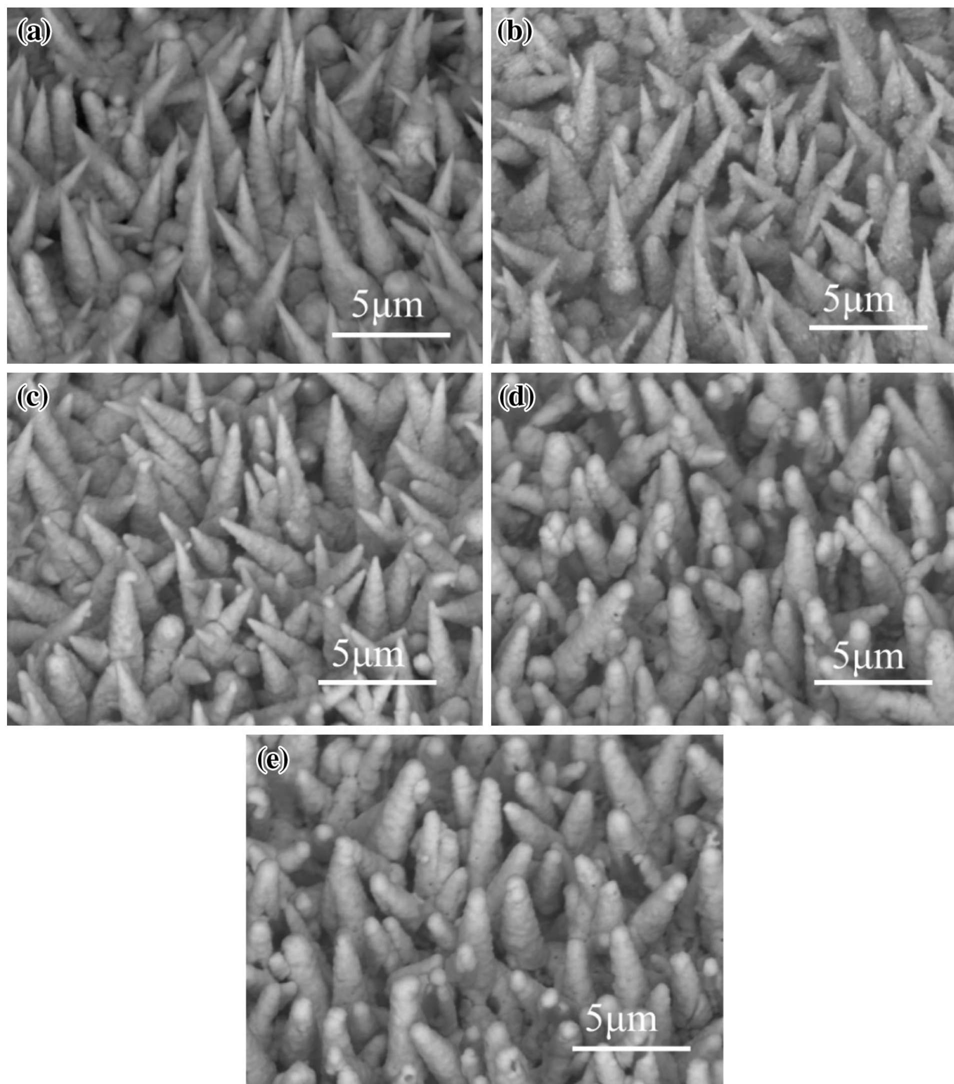

Fig. 2. SEM images of Cu microcones with Ag layer for different deposition times of (a) 0 min, (b) 6 min, (c) 12 min, (d) 18 min, and (e) 24 min.

surface of the substrate and the reaction stopped immediately when the surface was completely covered by the metal, hence the coating thickness increased slowly, finally tending to be stable.

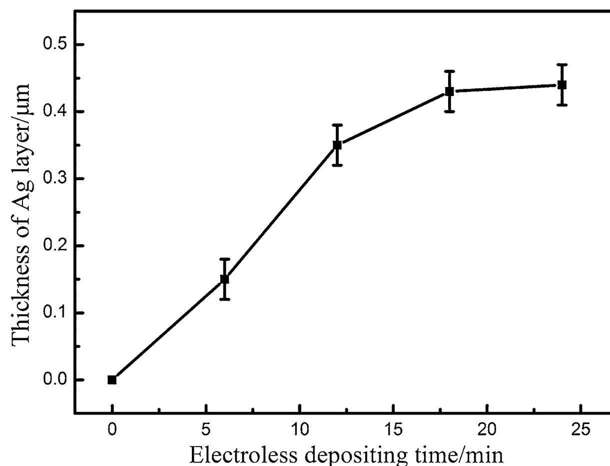

Fig. 3. Thickness of Ag layer on top of Cu microcones versus electroless deposition time.

Oxidation Behavior

In this experiment, CuO and Cu_2O cannot be completely separated due to experimental limitations and other conditions. Taking into account the oxidation at low temperature for a short time, we assume the use of simple Cu_2O in the calculation of copper oxidation to be reasonable. Moreover, there are many reports on the oxide phase; For example, Mayer carried out a detailed study on oxidation of copper and copper alloy thin films.[13] It was reported that copper is first oxidized to Cu_2O at 200°C and then to CuO at 300°C near the copper surface.

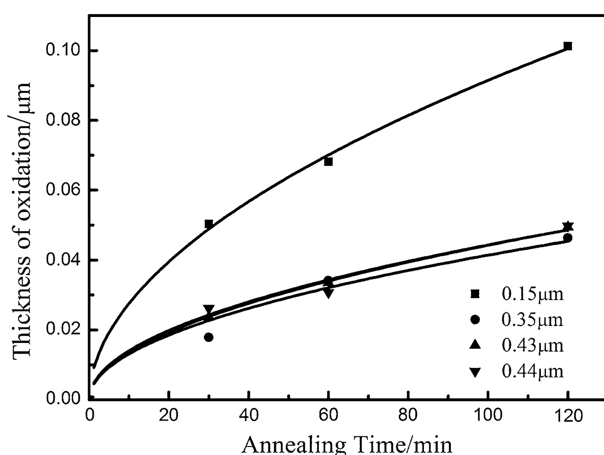

Fig. 4. Thickness of oxide layer of Cu microcones with Ag layer versus annealing time at 463 K.

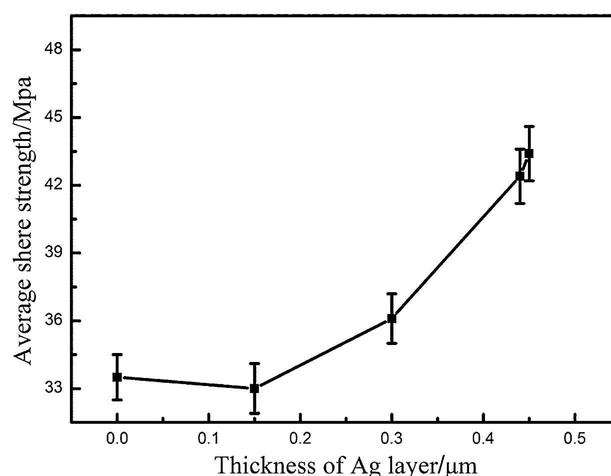

Fig. 5. Shear strength of bonded joints versus thickness of Ag layer on the top of Cu microcones.

Based on a large number of experiments, researchers have collated knowledge on metal oxidation in the form of kinetic curves. A kinetic curve for metal oxidation generally exhibits a straight, parabolic, cubic, logarithmic, or antilogarithmic form. The dynamics of oxidation of the same metal may follow different rules at different temperatures. Generally speaking, copper conforms to a logarithmic rule for thin oxide films at low temperature.[17–19]

The oxide thickness on the Cu microcones coated with Ag for different oxidation times and temperatures is shown in Fig. 4.

Figure 4 shows the copper oxide film thickness for the different electroless plated silver coatings under the condition of 463 K. As can be seen from this graph, with increasing annealing time, the oxide film thickness gradually increased. When the thickness of the silver plated layer reached 0.35 μm, the rate of increase of the oxide film thickness with increasing aging time slowed significantly. This phenomenon illustrates that Cu microcones with a Ag layer have a certain antioxidant effect. Curve-fitting results also showed that the oxide film thickness of the copper microcones coated with Ag fully complied with a logarithm growth law, as obtained in previous research.[18]

This logarithmic law can be partially explained by a number of factors. With increasing thickness of the oxide film, it becomes tighter. This indicates that the outer layer of the film has enormous elastic compressive stress during its growth, slowing down the diffusion rate of oxygen, combined with the instability of diffusion conditions, resulting in a slower oxidation rate.

Low-Temperature Solid-State Bonding by Ag-Coated Cu Microcones

The average shear strength of bonded joints obtained with a Ag layer of different thicknesses on top of Cu microcones for bonding pressure of 1000 g and time of 3 min is presented in Fig. 5. Each average shear strength value was calculated from eight solder joints. The average shear strength was 33.5 MPa, 33.0 MPa, 36.1 MPa, 42.4 MPa, and 43.4 MPa for silver thickness of 0 μm, 0.15 μm, 35 μm, 0.43 μm, and 0.44 μm. As one can see from Fig. 5, the overall bonding performance of the copper microcones with the silver coating was better than for silver-free ones in hot pressure welding. The average shear strength gradually increased as the thickness of the silver layer was increased. However, the average shear strength of the solder joints did not exhibit any obvious change until the thickness of the Ag layer reached 0.43 μm. This shows that, when the oxide film thickness decreased with the electroless silver coating on the copper microcones, the bonding time was short and a lot of intermetallic compounds were generated. Therefore, the average shear strength of the solder joint increased. Based on the above discussion, the best bonded samples were those using Cu microcones with 0.43 μm Ag coating.

Figure 6 shows cross-sectional SEM images of bonded joints formed at the bonding condition of 1000 g and 3 min with a Ag layer. From the interfacial images, we can see that the tips of the Cu microcones are wholly immersed in the solder matrix (as shown in Fig. 6a and b). Meanwhile, a thin, bright layer appears along the interface. This bright layer is probably intermetallic compound, but is under investigation and will be reported later. There are few voids at the interface under this bonding condition, indicating the formation of a compact bonded structure.

The elemental distribution shown in Fig. 6c was measured along the 40-μm black vertical line marked in Fig. 6a. The main composition of the Cu microcones was copper, whereas the main components of the solder were accompanied by a small amount of silver. At the interface between the two,

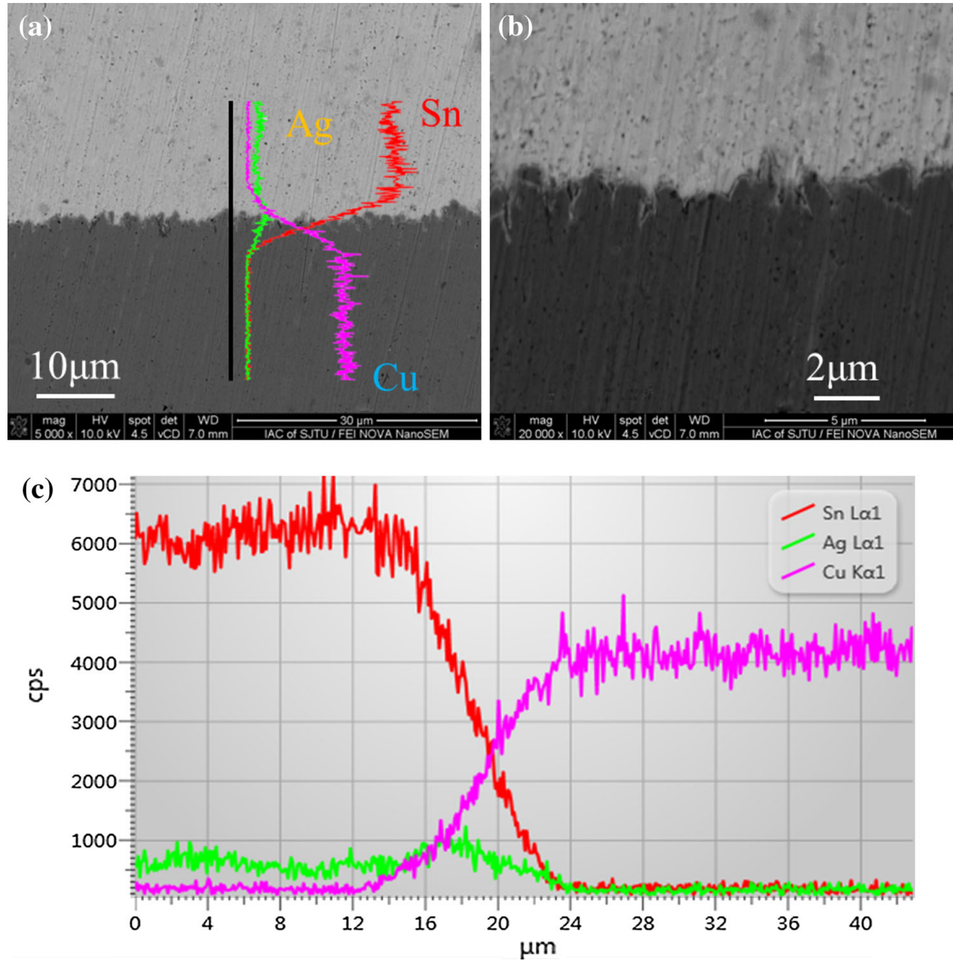

Fig. 6. (a, b) Cross-sectional SEM images of bonded joints with 0.15 μm Ag layer; (c) EDS results of bonded joints.

however, a thick layer of silver could be detected. Ni cone insertion bonding performed by Geng et al.[20] also showed that solid-state diffusion was a key element in this insertion bonding process.

For comparison with Fig. 6, Fig. 7 shows cross-sectional and EDS images for Cu microcones with a 0.43-μm Ag layer. Larger insertion bonding and less holes are observed. Because of the special morphology of the copper microcones, the silver elemental content shows minor fluctuations, reflecting that solid-state diffusion occurs during the bonding process. With Brinell hardness of 25 for silver and 37 for copper, the surface of the copper microcones coated with a softer layer of silver filled some gaps at the bases of the copper microcones, being advantageous for solder–substrate bonding.

After the ball shear test, micrographs of the fracture surfaces were studied. Figure 8 shows the fracture surface of the Cu microcone side for the bonding condition of 190°C and 1000 g. Compared with Fig. 8a and c, it can be easily found that more solder remains on the surface of the Cu microcones coated with 0.43 μm of Ag than for those coated with 0.15 μm of Ag after shear testing. The plated silver layer exhibits a more uniform contact and larger area between the solder and copper microcones, leading to an enhanced average shear strength, while only part of the Cu microcones coated with 0.15 μm of Ag form close connection with the solder. This also verifies the above conclusion that the silver layer reduces the formation of the oxide film, filling some gaps between the bases of the copper microcones, which is conducive for effective solder–substrate bonding. Figure 8b and d shows that fracture took place inside the solder rather than at the interface during the shear test.

IMC Morphology

To study the solid-state interfacial reactions between the solder and Cu microcones, a Sn layer was electrodeposited to investigate a void-free bonded sample. Figure 9 shows top-view SEM micrographs of such Sn/Ag/Cu microcone diffusion samples aged at 463 K for 3 min, 5 min, 9 min, 16 min, 25 min, and 36 min with the Sn layer etched by 10 vol.% HNO_3. As shown in Fig. 9a, in the diffusion samples, after annealing for 3 min,

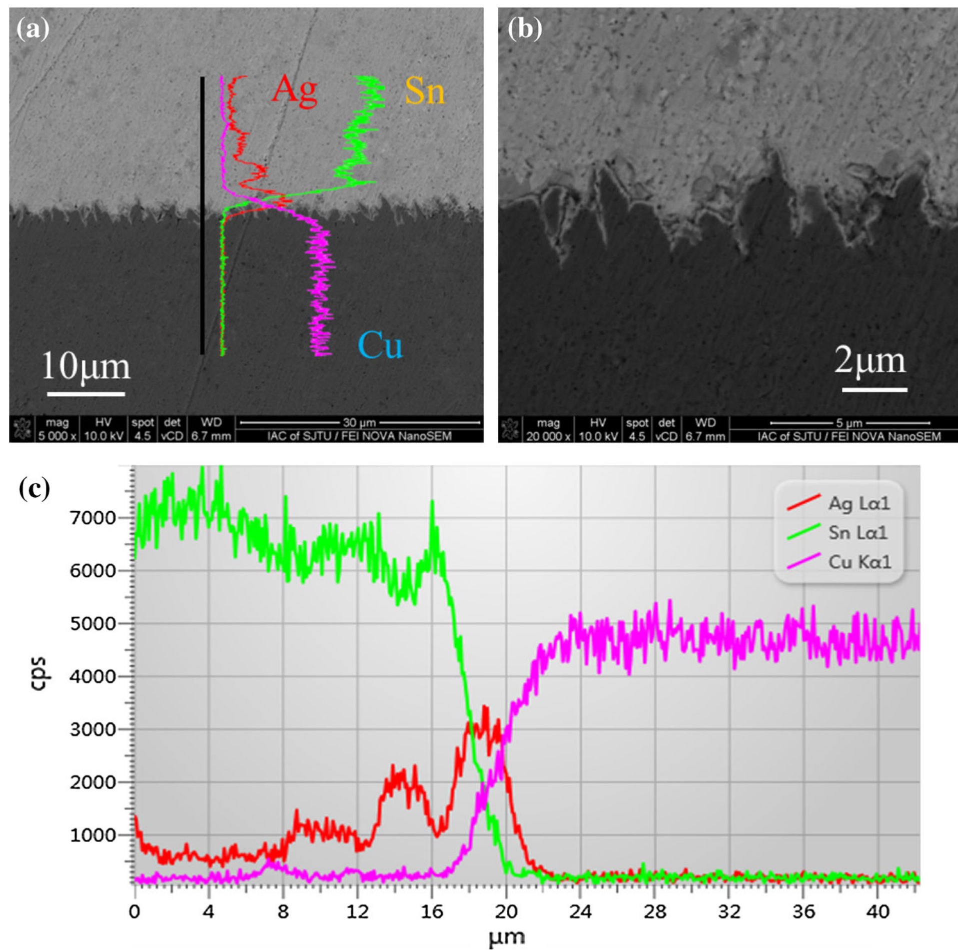

Fig. 7. (a, b) Cross-sectional SEM images of bonded joints with 0.15-μm Ag layer; (c) EDS results of bonded joints.

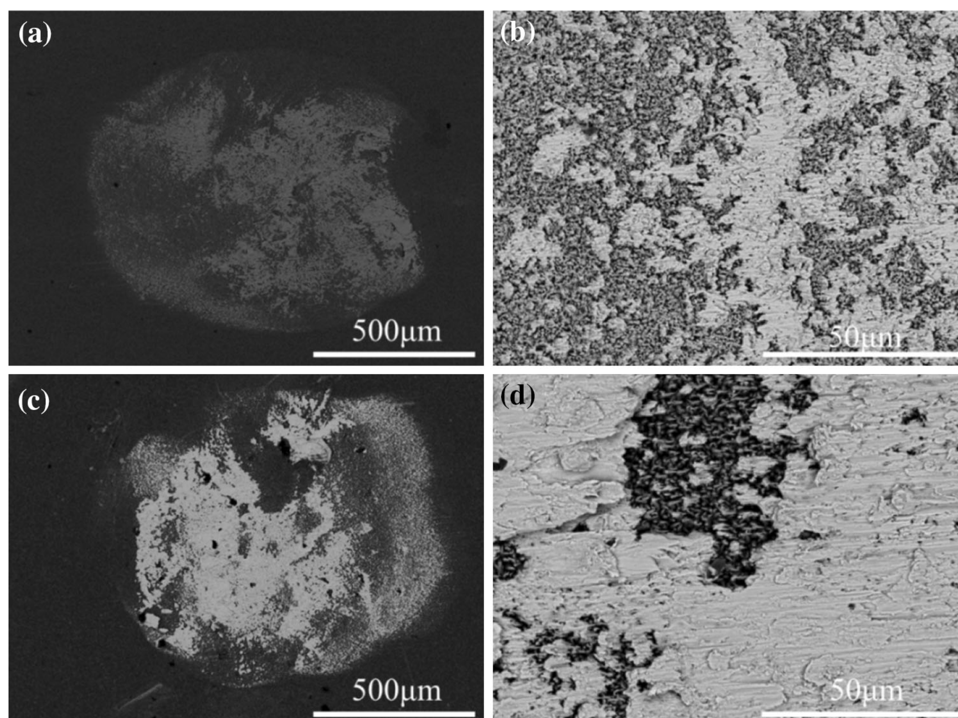

Fig. 8. Fracture observation of bonded joints with surface Ag layer: (a, b) Cu/0.15μm Ag; (c, d) Cu/0.43μm Ag.

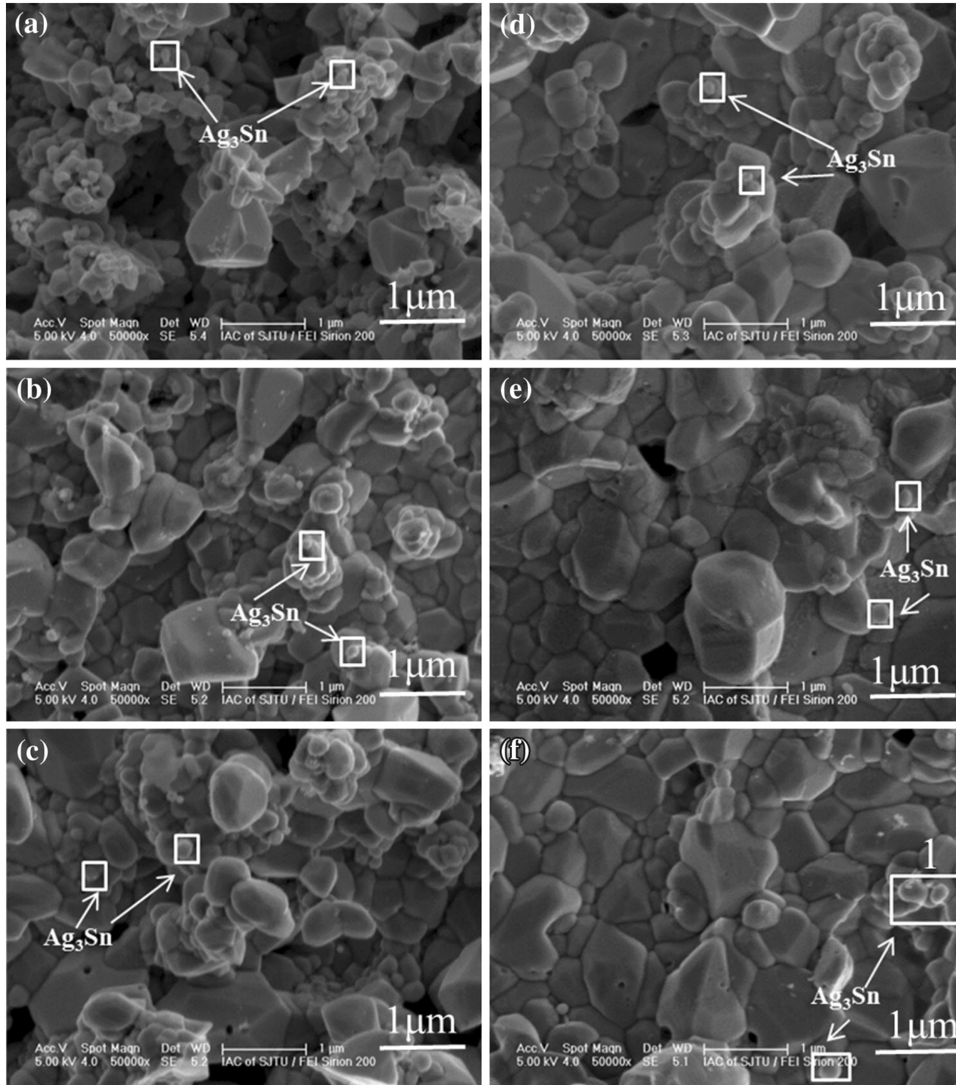

Fig. 9. SEM top-view images for Sn/Ag/Cu microcone diffusion samples annealed for (a) 3 min, (b) 5 min, (c) 9 min, (d) 16 min, (e) 25 min, and (f) 36 min at 463 K with Sn layer etched.

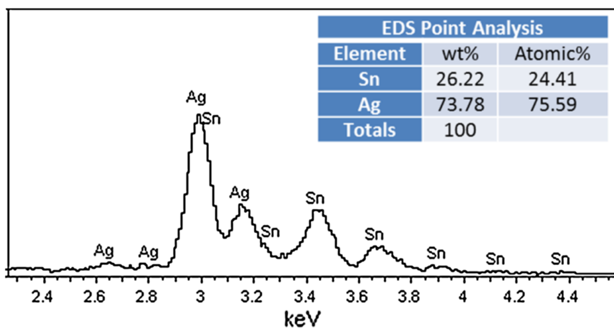

Fig. 10. EDX results for Fig. 9f.

nucleation started to occur at the boundary between the Sn and Cu microcones, with some grains forming at the top of the microcones. According to the XRD results, the grains were proved to be Cu_6Sn_5. As the annealing time was increased, the Cu_6Sn_5 grains grew larger and began to form clusters. With increased annealing time of 36 min, as seen in Fig. 9f, the grain size reached 1 μm. Similar results have been reported in literature.[21] Besides, many nanosized particles were found on the IMC surface. From the EDS (Fig. 10) point analysis of such particles, the ratio of Ag to Sn was 3:1, providing proof of the presence of Ag_3Sn. XRD analysis also revealed that these particles were Ag_3Sn, as discussed below.

Figure 11 shows the x-ray diffraction patterns of the Sn/Ag/Cu microcone diffusion samples, demonstrating the presence of Cu, Cu_6Sn_5, and Ag_3Sn. Four strong diffraction peaks near 43°, 50°, 74°, and 90°, respectively, correspond to the (111), (200), (220), and(311) planes of Cu according to Joint Committee on Powder Diffraction Standards (JCPDS) file no. 040836, while three apparent peaks (one near 30° and two near 43°) were found and

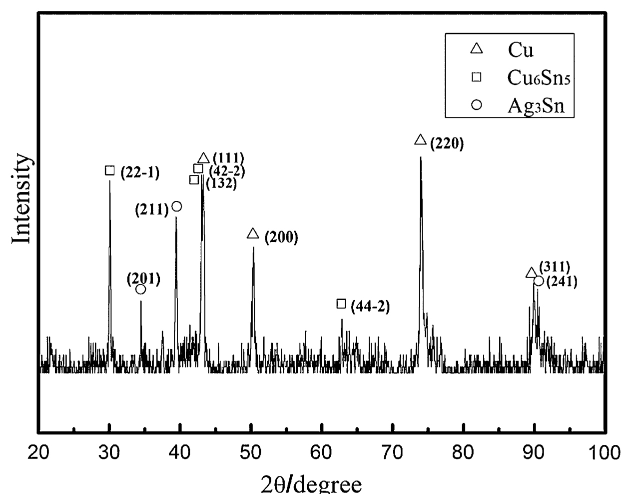

Fig. 11. XRD patterns of Sn/Ag/Cu microcone diffusion samples annealed for 36 min at 463 K with Sn layer etched.

Fig. 12. Schematic diagram of interfacial void disappearance.

could be indexed to the (22-1), (132), and (42-2) planes of Cu_6Sn_5, respectively (JCPDS file no. 451488). Cu_6Sn_5 has two major peaks at 42.97° and 43.27° while Cu has one major peak at 43.29°, making identification by XRD analysis difficult. One weak peak at around 63° corresponds to diffraction from the Cu_6Sn_5 crystal plane (42-2). In addition to the strong peak, diffraction peaks from Ag_3Sn could also be found at 2θ = 35°,40°, and 90°, which could be indexed to the (201), (211), and (241) planes (JCPDS file no. 441300).

Based on the above discussion, the average shear strength of Ag-coated Cu microcones was larger than for bare Cu microcones after the same bonding condition. This is assumed to be mainly due to the difference in the diffusion and oxidation rates between Ag and Cu. As the interdiffusion coefficient of Ag in Sn (1.9×10^{-17} cm^2 s^{-1}) at room temperature is larger than that of Cu in Sn (6.6×10^{-17} cm^2 s^{-1}),[22–24] Ag and Sn may diffuse very fast in each other on contact, resulting in formation of a strong bond between Ag and Sn. In atmospheric air, Cu is oxidized more easily, so a thicker oxide layer and a relatively lower diffusion rate might decrease the bond strength. Meanwhile, Ag_3Sn attached to the Cu_6Sn_5 at the solder joint interface, which could realize dispersion strengthening and enhance the adhesive strength.[25] This occurs because, at preferential sites, the effective surface energy is lower, thus diminishing the free energy barrier and facilitating nucleation. Finally, silver is softer than copper and free to escape by plastic flow to the sides of the Cu microcones during the hot pressure insertion bonding process, which contributes to the disappearance of the voids as shown in Fig. 12.

CONCLUSIONS

The influence of the thickness of the oxide layer on Cu microcones with a Ag layer for different annealing times was investigated. After the silver layer thickness reached 0.43 μm, the morphology of the copper microcones did not change and the rate of increase of the oxide film with increasing aging time slowed down significantly. Sn-based solder/Ag-coated Cu microcone solid-state bonding at low temperature was developed and evaluated at ambient atmosphere for 3D integration. Results of SEM and EDS investigations illustrated that the bonds exhibited good characteristics, with compact insertion of the two metals. The average shear strength was improved with the electroless silver coating.

As the silver layer protects the Cu microcone surface from contamination and oxidation and Ag_3Sn attached to the Cu_6Sn_5 at the solder joint interface within a short annealing time, contributing to the enhanced shear strength, better bonding quality resulted. These results demonstrate that Ag/Cu microcone bonding technology has great potential for use in low-temperature 3D integration applications.

ACKNOWLEDGEMENTS

This work is sponsored by the National Natural Science Foundation of China (61176097, 61376107) and the National Basic Research Program of China (973 Program, 2015CB057200). We also thank the Instrumental Analysis Center of Shanghai Jiao Tong University for use of SEM/EDS equipment.

REFERENCES

1. J. Kim and C.C. Lee, *Mater. Sci. Eng. A* 448, 345 (2007).
2. Y.-S. Chien, Y.-P. Huang, R.-N. Tzeng, M.-S. Shy, T.-H. Lin, K.-H. Chen, C.-T. Chuang, W. Hwang, J.-C. Chiou, C.-T. Chiu, H.-M. Tong, and K.-N. Chen, In *2013 IEEE 63rd Electronic Components and Technology Conference, ECTC 2013, May 28, 2013–May 31, 2013*, (Las Vegas: Institute of Electrical and Electronics Engineers Inc., 2013), p. 1146.
3. A. He, T. Osborn, S.A.B. Allen, and P.A. Kohl, *Electrochem. Solid-State Lett.* 9, 192 (2006).
4. R.I. Made, C.L. Gan, L. Yan, K.H.B. Kor, H.L. Chia, K.L. Pey, and C.V. Thompson, *Acta Mater.* 60, 578 (2012).
5. C.-T. Ko, and K.-N. Chen, *Microelectron. Reliab.* 52, 302 (2012).
6. B. Swinnen, W. Ruythooren, P. De Moor, L. Bogaerts, L. Carbonell, K. De Munck, B. Eyckens, S. Stoukatch, D. Sabuncuoglu Tezcan, Z. Tokei, J. Vaes, J. Van Aelst, and E. Beyne, In *2006 International Electron Devices Meeting, IEDM, December 10, 2006–December 13, 2006*, (Institute of Electrical and Electronics Engineers Inc.: San Francisco, CA, 2006), IEEE Electron Devices Society.
7. E.-J. Jang, S. Hyun, H.-J. Lee, and Y.-B. Park, *J. Electron. Mater.* 38, 2449–2454 (2009).
8. W. Zhang, X. Feng, H. Cao, H. Anmin, and M. Li, *Appl. Surf. Sci.* 258, 8814–8818 (2012).
9. Z. Chen, T. Luo, T. Hang, M. Li, and H. Anmin, *ECS Solid State Lett.* 1, P7 (2012).

10. Z. Chen, T. Luo, T. Hang, M. Li, and H. Anmin, *CrystEngComm* 15, 10490 (2013).
11. L. Qin, Z. Chen, W. Zhang, H. Anmin, and M. Li, *Appl. Surf. Sci.* 268, 368 (2013).
12. R. Berriche, R. Lowry, and M. I. Rosenfield, in *International Symposium on Advanced Packaging Materials: Processes, Properties and Interfaces, 1999.* IEEE (1999).
13. J. Li, W. Mayer, and E.G. Colgan, *J. Appl. Phys.* 70, 2820 (1991).
14. G.G. Jernigan, and G.A. Somorjai, *J. Catal.* 147, 567 (1994).
15. W. Zhang, Y. Zheyin, Z. Chen, and M. Li, *Mater. Lett.* 67, 327 (2012).
16. Q. Zhao, H. Anmin, M. Li, and J. Sun, *Microelectron. Reliab.* 53, 321 (2013).
17. T.N. Rhodin Jr, *J. Am. Chem. Soc.* 72, 5102 (1950).
18. W.E. Campbell, and U.B. Thomas, *Trans. Electrochem. Soc.* 76, 303 (1939).
19. M. Sanchez, J. Rams, and A. Urena, *Oxid. Metals* 69, 327 (2008).
20. W. Geng, Z. Chen, H. Anmin, and M. Li, *Mater. Lett.* 78, 72 (2012).
21. Y. Huang, T. Hang, H. Anmin, Z. Chen, L. Qin, and M. Li, *J. Alloy. Compd.* 582, 408 (2014).
22. Ž. Marinković, and V. Simić, *Thin Solid Films* 217, 26 (1992).
23. B.F. Dyson, *J. Appl. Phys.* 37, 2375 (1966).
24. K. Suzuki, S. Kano, M. Kajihara, N. Kurokawa, and K. Sakamoto, *Mater. Trans.* 46, 969 (2005).
25. H.-T. Lee and Y.-H. Lee, *Mater. Sci. Eng. A* 419, 172 (2006).